ELECTRON CYCLOTRON MEASUREMENTS IN THE W VII-A STELLARATOR

A. Cavallo, M. Tutter

IPP 2/244 Dezember 1978

MAX-PLANCK-INSTITUT FÜR PLASMAPHYSIK

8046 GARCHING BEI MÜNCHEN

MAX-PLANCK-INSTITUT FÜR PLASMAPHYSIK

GARCHING BEI MÜNCHEN

ELECTRON CYCLOTRON MEASUREMENTS IN THE W VII-A STELLARATOR

A. Cavallo, M. Tutter

IPP 2/244 Dezember 1978

Die nachstehende Arbeit wurde im Rahmen des Vertrages zwischen dem Max-Planck-Institut für Plasmaphysik und der Europäischen Atomgemeinschaft über die Zusammenarbeit auf dem Gebiete der Plasmaphysik durchgeführt.

IPP 2/244 A. Cavallo +)
M. Tutter

Electron Cyclotron Measurements on W VII-A

(December 1978, in English)

ABSTRACT

Transmission and emission measurements of radiation at the electron cyclotron harmonics have been carried out on the plasma confined in the Wendelstein VII A Stellarator,using both broadband and narrowband techniques.

These show that it is possible to use the emission at the second cyclotron harmonic to obtain an electron temperature profile of the plasma. This has been done in real time using a Michelson interferometer of special design.

However, in contrast to the results on PLT and TFR, emission at the first harmonic cannot be used to measure the electron temperature on W VII A. This radiation is not at the blackbodylevel and appears to contain features not associated with electron cyclotron resonance emission.

Also, transmission measurements show an anomalous absorption at the second harmonic ordinary polarization, which should be more carefully investigated. These measurements also indicate that the theoretically predicted absorbtion at the first harmonic ordinary polarization does take place, making electron cyclotron resonance heating a definite possibility.

+) Centre d'Etudes Nucléaires de Fontenay-aux-Roses
Service de Confinement des Plasmas

I - INTRODUCTION

In a magnetically confined hot plasma, electrons gyrate around magnetic field lines, radiating energy. It has been shown that in addition to this radiation being a significant energy loss mechanism for very hot plasmas (1,2), detailed measurement of this radiation could yield important information on the local density and temperature of the plasma (3). Also, the development of the gyrotron (4) as a high power source of millimeter radiation (200 kW, 85 GHz), has made feasible electron cyclotron resonance heating of a plasma confined in a 30 kG magnetic field. It is therefore of fundamental importance to study the propagation in a hot plasma of radiation at the first and second cyclotron harmonics.

These experiments were done on the Wendelstein VII A Stellarator (5), major radius 200 cm, plasma radius 10 cm, which has an $l = 2$, $m = 5$ helical winding giving an almost shearless rotational transform $0.055 \leqslant \tau \leqslant 0.23$ with a toroidal field $B \leqslant 3.5$ T.

The toroidal field decreases with increasing major radius, and thus the electron cyclotron frequency $f_N = \frac{N}{2\pi} \frac{q}{m} B(R)$, also decreases with increasing radius. Here N is the harmonic number, $\frac{q}{m}$ is the charge to mass ratio of the electron and B(R) is the local toroidal magnetic field. This assumes that the contribution of the current in the helical windings and the plasma current to the local magnetic field can be ignored, which is quite reasonable.

The width of the individual lines in the spectrum is determined by the total change in the toroidal magnetic field across the plasma column. For W VII A, total line width is about 10 %. For example, at a toroidal field of 25 kG, the width of the second harmonic (F = 140 GHz) is about 14 GHz. This is much narrower than the line width of electron cyclotron radiation from a tokamak, which has a much larger ratio of plasma diameter to toroidal radius. In addition, the electron temperature in a stellarator is lower than that in tokamak ($T(r = 0) \approx 500$ eV in W VII A). This means that a high resolution is needed for these measurements, and that there is relatively little power available in the spectrum.

A Michelson interferometer, which has a resolution proportional to mirror displacement, will need a large displacement to resolve the spectral lines. However, a bandwidth of 14 GHz at 140 GHz is quite large for a swept superheterodyne receiver, while a FabryPerot is difficult to use because of the lack of sensitivity in the available detectors (6). Consequently it is difficult to measure the electron cyclotron radiation spectrum under these conditions.

II - THEORETICAL CONSIDERATIONS

The specific intensity of the emitted radiation I (watts per square meter per steradian per radian frequency interval) is given by Kirchoff's radiation law as :

$$I = \frac{\omega^2}{8\pi^3 c^2} \; k\, T_e \; (1 - e^{-\tau})$$

Here ω is the frequency of the radiation, c the speed of light, $k\, T_e$ the electron energy and τ the optical depth of the medium. The back body intensity is $I_b = \frac{\omega^2}{8\pi^3 c^2} \; k\, T_e$. When the optical depth of the plasma is greater than about 2, the plasma radiates and absorbs as a black body and the electron temperature as a function of radius is obtained simply by measuring the power emitted by the plasma as a function of frequency. Under this condition, this is a local measure of the plasma temperature. Thus, a knowledge of the optical depth of the plasma is of great importance both for diagnostic purposes as well as for potential heating applications.

The optical depth for radiation at the second harmonic, extraordinary polarization (wave electric field $\vec{E}$ perpendicular to magnetic field $\vec{B}$) is given by (3) (only propagation along the major radius is considered here) :

Eq. 1 $$\tau_{EO,2} = \pi^2 \frac{\omega_p^2}{\omega_c^2} \left(\frac{k\, T_e}{mc^2}\right) \frac{R}{\lambda}$$

Here ω_p is the plasma frequency, ω_c is the electron cyclotron frequency, λ is the wavelength of the radiation and R is the major radius of the torus. For Wendelstein VII A, ($k\, T_e \simeq 500$ eV, $N_e \simeq 3 \times 10^{13}$), $\tau_{EO,2} = 2\text{-}3$, and this harmonic is quite interesting for diagnostic purposes.

For the ordinary polarization ($\vec{E}$ parallel to $\vec{B}$), (7),

Eq. 2 $$\tau_{0,2} = \pi^{\frac{3}{2}} \left(1 - \frac{\omega_p^2}{\omega_c^2}\right) \left(\frac{k\, T_e}{mc^2}\right)^2 \frac{R}{\lambda} \approx 3 \times 10^{-3}$$

and the plasma should be transparent for this radiation.

At the first harmonic, the optical depth for the extraordinary polarization ($\vec{E} \perp \vec{B}$) is (7,8) :

Eq. 3 $$\tau_{E0,1} = 2\sqrt{2}\ \frac{\omega_c^2}{\omega_p^2}\ \left(1 - \frac{1}{2}\cdot\frac{\omega_p^2}{\omega_c^2}\right)^{\frac{3}{2}}\ \left(\frac{k\ T_e}{mc^2}\right)^2\ \frac{R}{\lambda} \approx 5 \times 10^{-3}$$

for typical plasma parameters on W VII A.

However, measurements on the PLT and TFR tokamaks (9, 10) have clearly shown that emission at the first harmonic, extraordinary polarization is blackbody emission. This has been explained by postulating the conversion of electrostatic Bernstein waves into extraordinary electromagnetic waves at the electron cyclotron frequency. The optical depth for these electrostatic waves is given by (9) :

Eq. 4 $$\tau \approx 9\ \pi^3\ \left(\frac{\omega_p}{\omega_c}\right)^{\frac{2}{3}}\ \left(\frac{2\ k\ T}{mc^2}\right)^{\frac{1}{6}}\ \frac{R}{\lambda} \approx 10^4$$

Thus, this radiation could also be very interesting for diagnostic purposes.

The optical depth at the first harmonic, ordinary polarization is given as (7,8) :

Eq. 5 $$\tau_{0,1} = \pi^2\ \left(\frac{\omega_p^2}{\omega_c^2}\right)\ \frac{k\ T_e}{mc^2}\ \left(1 - \frac{\omega_p^2}{\omega_c^2}\right)^{\frac{1}{2}}\ \frac{R}{\lambda} \approx 1$$

This radiation is, therefore, not of great interest for diagnostic purposes ; but for plasma heating it is of primary importance.

This is due to the fact that the propagation characteristics of this radiation are affected by the presence of the plasma. This is illustrated in Figure 1. Regions of non-propagation for the radiation are cross-hatched. Radiation at the second harmonic is accessible from either the inside or the outside of the torus. However, at the first harmonic ($\vec{E} \perp \vec{B}$), there is a region of non-propagation between the electron cyclotron resonance region and the outside of the torus. To be measured correctly, this radiation must be observed with a horn mounted on the inside of the torus.

This is quite difficult for many tokamaks, and even for W VII A, and makes plasma heating using this polarization very difficult. This problem is not encountered for the ordinary polarization, making its use in heating experiments very attractive.

One other factor to be considered is the line width of the resonance, as distinguished from the total line width which corresponds to the electron temperature profile. If the emission is to be used as a measure of local electron temperature, not only must the local optical depth be larger than about 2, but also the line width must be narrow compared to the electron temperature profile.

The doppler broadening of the electron cyclotron radiation is given by :

$$\frac{\Delta f_d}{f} = \sqrt{2\pi}\ \left(\frac{k\ T_e}{mc^2}\right)^{\frac{1}{2}}\ N \cos\theta$$

Here N is the harmonic number and $\theta = \frac{\pi}{2}$ corresponds to a direction of observation along the major radius.

The relativistic broadening is :

$$\frac{\Delta f_r}{f} = \sqrt{2\pi N}\ \left(\frac{k\ T_e}{mc^2}\right)$$

For the aperature of the outer horn on the W VII A (superheterodyne system) and for the Michelson interferometer, the 3 dB point on the antenna pattern is about 4°. Thus the total line broadening is :

$$\Delta f = \sqrt{\Delta f_r^{\,2} + \Delta f_d^{\,2}} \approx 1\ \text{GHz}$$

at the second harmonic at 140 GHz. This implies a spatial resolution of at worst 1,4 cm, adequate for temperature profile measurements.

III - EXPERIMENTAL RESULTS : Superheterodyne measurements

The experimental arrangement for the superheterodyne measurements is shown in Figure 2. Emission and transmission could be measured simultaneously using horns mounted on the inside and the outside of the torus. The outer horn was matched to the plasma for frequencies around 150 GHz, while the inner horn was matched for frequencies around 75 GHz.

This means, if λ is the wavelength under consideration, Z the plasma antenna distance, A the maximum relevant dimension of the antenna and D the plasma diameter, that (11) : $\left[\begin{matrix}\lambda \\ \frac{A^2}{\lambda}\end{matrix}\right] \leqslant Z \leqslant \frac{AD}{2\lambda}$

The power received by the antenna under these conditions is directly proportional to the black body plasma temperature independent of frequency and antenna geometry.

These measurements were made at fixed frequency (138.4 GHz, second harmonic at B = 24.72 kG, and 72,5 GHz, first harmonic at B = 25.8 kG), observing along the major radius. The temperature profile (or, more correctly, emission line profile), was obtained by changing the value of the toroidal magnetic field, thus changing the location of the resonance region across the plasma column.

Results from these emission measurements are shown in Figure 3. Here, measurements made using the outer horn were compared with the signal obtained from the noise tube to obtain an absolute value of the electron temperature. The temperature profile obtained from these emission measurements agrees very well with that obtained from laser scattering. It had to be assumed that the toroidal field given by the control console was systematically larger than the true value by 325 G. Conversations with the technical staff of W VII A indicated that this was certainly a possibility, since the absolute value of the toroidal field in W VII A had never been measured to this accuracy.

The emission measured using the inner horn could not be calibrated absolutely. Therefore a single point on this curve was normalized to the Thomson scattering value of the electron temperature. The profile measured in this manner also agreed well with that measured by Thomson scattering and with emission measured using the outer horn. This agreement is to be expected theoretically, as mentioned previously.

The local electron density and temperature as determined by Thomson scattering were used to calculate the optical depth [from Eq. 1] of the plasma as a function of radius. The emission measurements indicate that the electron temperature profile can be recovered even if the optical depth of the plasma is much less than one, contrary to the expectation that $\tau \gtrsim 2$ for this measurement. This discrepancy is most likely explained by the high reflectivity of the vacuum wall increasing the apparent optical depth of the plasma (12).

For an optically thin plasma, $\tau \ll 1$, $e^{-\tau} \approx 1 - \tau$, the intensity of the emission is given by (assuming the emission in the ordinary and extraordinary modes is equal, as is the case for W VII A) :

$I = I_b \left(\frac{\tau}{1 - \rho(1 - \tau)}\right)$ where ρ is the wall reflectivity. For the frequencies of interest, $1 - \rho \simeq 10^{-2}$, and thus the plasma can appear to emit as a black body even if $\tau \simeq 10^{-1}$. The emission is then not a measure of local temperature, but an average for plasma at this radius in the entire torus. Such a measurement can still be very useful, however. The interpretation of such emission from plasma very close to the wall requires a better knowledge of the optical depth, which could be supplied from more accurate transmission measurements, for example.

Another set of experiments was done in which the transmission and emission of the plasma at the second harmonic, extraordinary polarization, were simultaneously measured.

The electron temperature profile obtained from the emission measurements agreed very well with that measured by laser scattering, both in the center of the plasma where the transmission is low and at the plasma edge where the transmission is quite high (> 50 %) (Figure 4). The local plasma density and temperature as determined by laser scattering were used to calculate the expected transmission from Eq. 1 (Figure 5). The fraction of power transmitted is given by $TR = e^{-\tau}$.

The measured transmission agrees reasonably well with these measurements, but may indicate that the optical depth is somewhat larger than predicted by Eq. 1 (13).

Measurements at the second harmonic ordinary polarization were also done (Figure 6). The temperature profile as determined from these emission measurements does not agree completely with the profile determined from extraordinary made emission or from laser scattering. Also, the transmission

is much smaller than that predicted from Eq. 2. This data must be checked more thoroughly, but may indicate that there is a larger than expected interaction between E ∥ B radiation and the plasma (12, 14).

Emission and transmission measurements were also made at the first harmonic, extraordinary polarization (Figure 7). The superheterodyne receiver was calibrated using a noise source ; for the inner horn it was assumed that the attenuation in the waveguide leading to the detector was the same as at 140 GHz. Since 8 mm oversized waveguide was used this is probably a reasonable assumption.

In contrast to results already mentioned on TFR and PLT, the electron temperature profile cannot be obtained from the emission measurements, and the emission is less than that expected from a thermal plasma. Also, the emission measured with the central field at 28-30 kG cannot be electron cyclotron radiation of thermal electrons, since at these fields the resonance region is located far outside the plasma column.

Emission measurements at the first harmonic, extraordinary polarization, using the outer horn on W VII A, were also made (Figure 8). These show that the emission is larger than what would be expected from a thermal plasma, and also show the non-cyclotron resonance radiation seen on the inner horn. The transmission behaves as would be expected with the presence of a non-propagating layer between the emitter and receiver, that is transmission is low when the resonance zone is in the center of the torus, and high when the resonance zone is outside the region between the two horns.

The transmission measured at the first harmonic, ordinary polarization (Figure 9) shows reasonable agreement when compared with the transmission predicted from Eq. 5, using local density and electron temperature measurements from laser scattering. (This indicates a very useful potential application in plasma heating). Once again, however, the level of the emission is much higher than that expected from a thermal plasma, and the emission shows non-cyclotron resonance features.

We do not have at present an explanation for the anomalous features of the electron cyclotron radiation at the first harmonic. A possible cause may be the presence of a small number of runaway or non-thermal electrons in the discharge. In many of the discharge studied, such effects were present in the first ten or twenty milliseconds of the discharge. These measurements were made at 100 milliseconds after the start of the discharge,

long after such effects had disappeared. The emission was essentially constant from t = 50 msec to the end of the discharge (t = 200 msec) for this series of experiments.

Unfortunately, the signal to noise ratio of the signals from the Michelson interferometer on W VII A was not adequate to allow a study of the emission at the first harmonic. This difficulty should shortly be corrected, enabling a comparison of results between the two methods and a more exact examination of the emission spectrum.

IV - EXPERIMENTAL RESULTS : Michelson Interferometer

A fast Michelson interferometer was also used to measure the electron cyclotron emission from W VII A. This was a polarization interferometer (12) with a moveable mirror driven by a pneumatic cylinder and a lever arm. The general mechanical scheme of this instrument is illustrated in Fig. 10A, while a block diagram of the electronics is shown in Fig. 10B. Details of the interferometer will be described elsewhere.

The resolution R of a Michelson interferometer is proportional to the mirror displacement d ($R = cd^{-1}$ where c is the speed of light) for a single sided interferogram. Since the second cyclotron harmonic will be of main interest for diagnostic purposes, it is useful to focus attention on the total line width of this harmonic, about 14 GHz at 140 GHz. To be of practical value, Michelson must have a resolution of about one-quarter of this, or a mirror displacement of about 5 cm. Furthermore, because of the low electron temperature and narrow line with of the cyclotron radiation from W VII A, the signal to noise ratio is only just adequate for these measurements. This is illustrated in Figure 11, which shows a typical interferogram taken on W VII A. It is therefore necessary to utilize a two sided interferogram to avoid having to locate the center of the interferogram. The maximum mirror speed attainable with the pneumatic cylinder-lever arm mechanism is about 16 m/sec., more than adequate to obtain the 10 cm mirror displacement in less than 10 msec.

The main portion of the interferogram is shown in Figure 12. It is characteristic of a spectrum dominated by a single strong narrow line, with some power in the higher and lower harmonics. A fast fourier transform done on the data, shows that this is indeed the case. This is just the spectrum one would expect from a thermal plasma (Figure 13).

The emission line at the second harmonic is enlarged and compared with the temperature profile measured with laser scattering (Figure 14). The agreement is reasonably good. It should be noted that the temperature profile obtained in this way is available immediately after each shot, in real time, via the computer terminal.

Also, the relatively unfavorable signal to noise ratio should be greatly improved in this next year (6). This will allow the use of a single sided interferogram, enabling the temperature profile to be obtained in one-half the time compared with the present arrangement, in addition to having much lower noise level.

V - SUMMARY AND CONCLUSIONS

The interferometer measurements show that for typical discharges on W VII A, the electron cyclotron radiation spectrum is thermal and the electron temperature profile can be obtained reliably, repeatedly and rapidly using a fast Michelson Interferometer.

Transmission and emission measurements made with the fixed frequency superheterodyne receivers have demonstrated that :

1. Second harmonic, $\vec{E} \perp \vec{B}$: Emission measurements can yield the electron temperature profile, in agreement with laser scattering measurements, using horns mounted on either the inside or outside of the torus.

2. Second harmonic, $\vec{E} \parallel \vec{B}$: Emission is at approximately the thermal level, and transmission is lower than expected. Further work is required to clarify this, in particular the transmission measurements should be carefully checked. These indicate an unexpected interaction between this radiation and the plasma.

3. First harmonic, $\vec{E} \perp \vec{B}$: Emission shows non -electron cyclotron features ; inner horn, emission is less than expected for a thermal plasma; outer horn, emission is larger than expected.

4. First harmonic, $\vec{E} \parallel \vec{B}$: Emission shows non-electron cyclotron features and is larger than expected from a thermal plasma. Transmission measurements show reasonable agreement with theory. Radiation at the first harmonic, ordinary or extraordinary polarization, cannot be used for diagnostic purposes on W VII A. The fact that first harmonic, ordinary polarization radiation is absorbed by the plasma, as predicted theoretically, indicates that an electron cyclotron resonance heating experiment on W VII A is a very interesting possibility.

ACKNOWLEDGEMENTS

The drafting and supervision of the machine-shop work for the large interferometer was done by Egon Katzmarek, who also made very valuable suggestions concerning the details of construction.

Technical support from the machine shop, in particular from Mr. Mauermair, and the assistance of Mr. Breitel, were most welcome. The laser group provided the electron temperature and density measurements.

D.W. Kerst and Bob Beck of the University of Wisconsin generously provided drawings from Wisconsin Toroidal Octupole for use on the large interferometer. Helpful conversations with Paul Nonn, of the University of Wisconsin, are also acknowledged.

REFERENCES

1. B.A. Trubnikov, V.5, Kudryavtsev, 2nd Int. Conf. Peaceful Uses of Atom. Energy (Proc. Conf. Geneva 1958) 31, 93 (1958).

2. M.N. Rosenbluth, Nucl. Fusion 10, 340 (1970).

3. I. Engelmann, M. Curatolo, Nucl. Fusion 13, 497 (1973)

4. V.A. Flyagin, A.V. Gaponov, M. I. Petelen, V.K. Yulpatov, IEEE, Trans. on Microwave Theory and Tech. 25, 514 (1977)

5. W VII A Team, Seventh Int. Conf. on Plasma Phys. and Controlled Thermonuclear Fusion, Innsbruck, Austria, Paper IAEA CN-37-H-2

6. New detectors recently developed may change this situation. See, for example, F. Nakajima, M. Kobayashi, S. Narita, Japanese J. of App. Phys., 17, 149 (1978), or the detectors from QMC instruments Ltd, 229 Mile End Road. London, E1 4AA

7. Y. M. Dnestrovskii, D.P. Kostomarov, M. V. Skrydlov, Soviet Physics, Technical Physics, 8, 691 (1964)

8. L. Fidone, S. Granata, I. Ramponi, R.L. Meyer, Phys. Fluids 4, 645 (1978)

9. J. Hosea, V. Arunasalam, R. Cano, Phys. Rev. Lett. 39, 408 (1977).

10. R. Cano, Private Communication.

11. M. A. Heald, C.B. Wharton, Plasma Diagnostics with microwaves ch. 7, John Wiley Sons, N.Y.C. 1965.

12. A.E. Costley, R.J. Hastie, J.W. M. Paul, J. Chamberlain, Phys. Rev. Lett. 33, 758 (1974)

13. E.B. Meservey, S.P. Schlesinger, Phys. of Fluids 8, 500 (1965).

14. I.H. Hutchson, D.S. Komm, Nuclear Fusion. 17, 1077 (1977).

FIGURE CAPTIONS

Figure 1 Radial Profiles of Characteristic Frequencies, Extraordinary Polarization, Using Measured Density Profiles
(N_e - 3.2 - 1.0 x $10^{13}/cm^3$)
F_p - Plasma Frequency
F_c, $2F_c$ - First + second Cyclotron Harmonic, B = 2.589 T
$F_{UH} = (F_p^2 + F_c^2)^{\frac{1}{2}}$ - Upper Hybrid Frequency

$F_{L,UCO} = \pm \frac{F_c}{2} + [(\frac{F_c}{2})^2 + F_p^2]^{\frac{1}{2}}$ - upper, lower cut-off frequency

Regions of non-propagation cross-hatched

Figure 2 Experimental Set-up for Superheterodyne Measurements

Figure 3 Emission Measurements, Second Harmonic, E ⊥ B, Inner and Outer Horn.

Figure 4 Emission and Transmission at the Second Harmonic, E ⊥ B.

Figure 5 Transmission at Second Harmonic, E ⊥ B, compared with Theory.

Figure 6 Transmission and Emission at the Second Harmonic E ∥ B.

Figure 7[+)] Emission and Transmission at the First Harmonic, E ⊥ B, Inner Horn.

Figure 8[+)] Emission and Transmission, First Harmonic, E ⊥ B, Outer Horn.

Figure 9[+)] Emission and Transmission, First Harmonic E ∥ B, Outer Horn.

[+)] It should be remembered that the emission has been measured as a function of the magnetic field B, and that the radius has been calculated from the inhomogeneity of B across the torus as the point where the electron cyclotron frequency equals the measuring frequency. Any radiation beyond the limiter radius therefore cannot be cyclotron radiation of thermal electrons.

Figure 10 Michelson Polarization Interferometer, Showing (A) Mechanical and (B) Electronic Block Diagrams.

Figure 11 Interferogram taken with the Interferometer (10 cm mirror displacement in 10 msec)

Figure 12 Main Portion of the Interferogram, Enlarged

Figure 13 Fast Fourier Transform of Interferogram, Showing Power Spectrum of Radiation.

Figure 14 Enlargement of Power vs Frequency Measured via the Interferometer, (compared with laser scattering measurements).

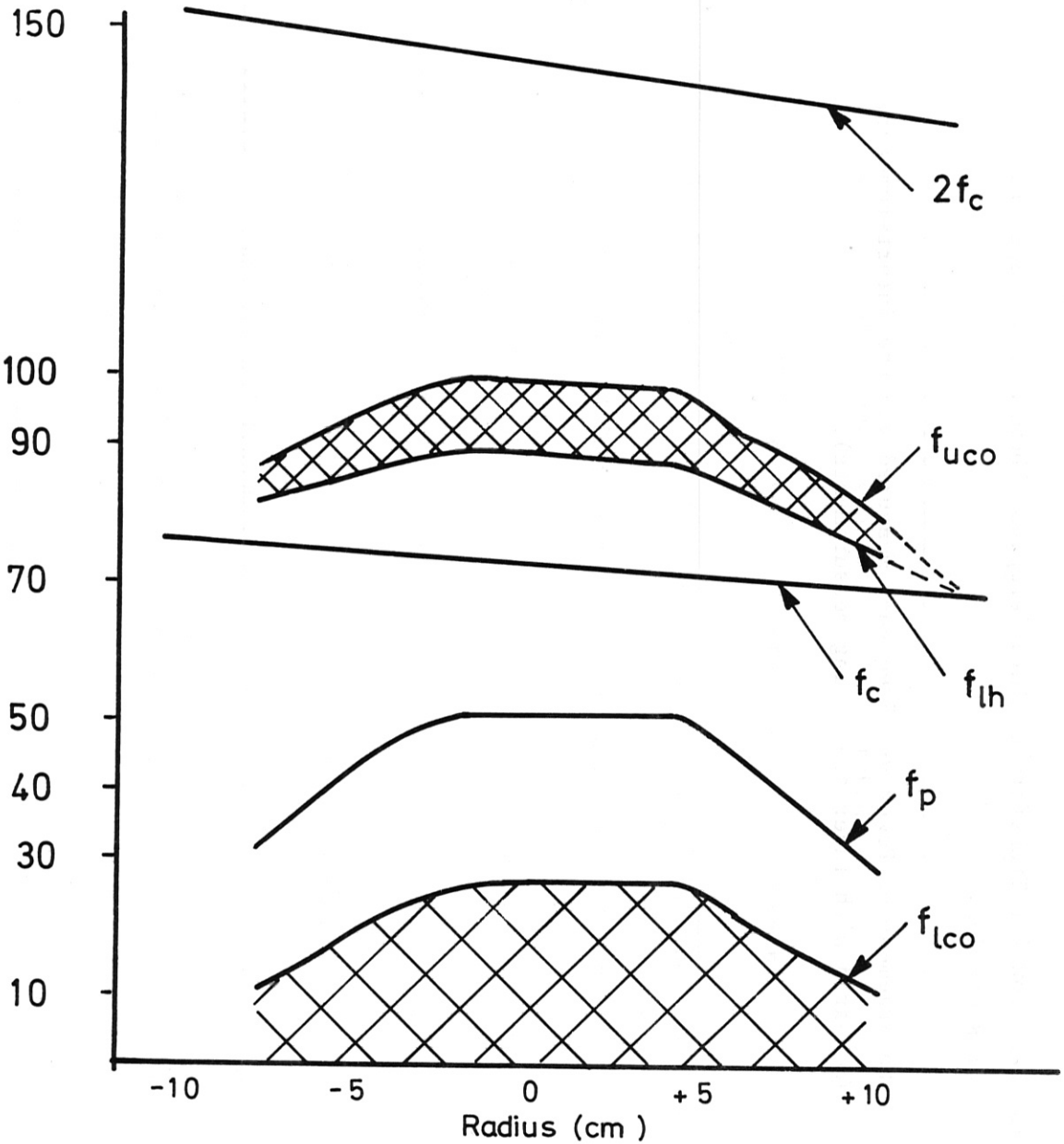

Figure 1

RADIAL PROFILES OF CHARACTERISTIC FREQUENCIES FOR E ⊥ B NON PROPAGATION CROSSHATCHED

B (r = 0) = 2,589 T N = 3,2 - 1x10^{13}/cm^3

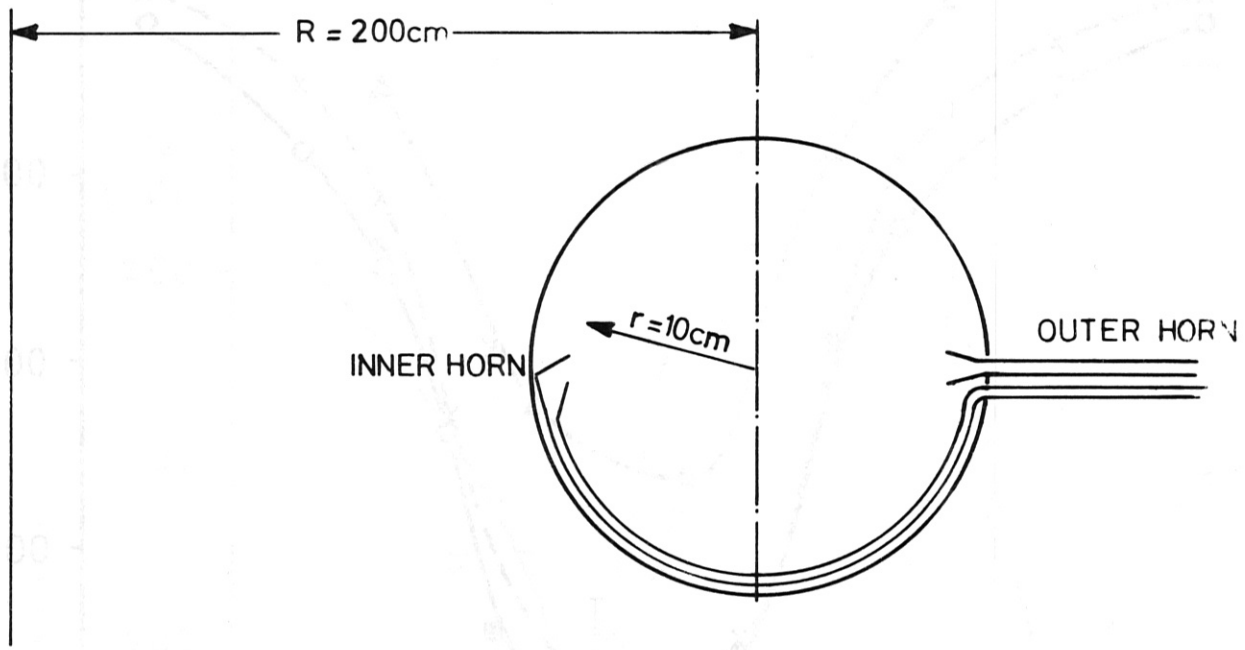

72,5 GHz Source

72,5 GHz Superheterodyne Receiver

138,4 GHz Superheterodyne Receiver

138,4 GHz Source

Figure 2

EXPERIMENTAL SET UP

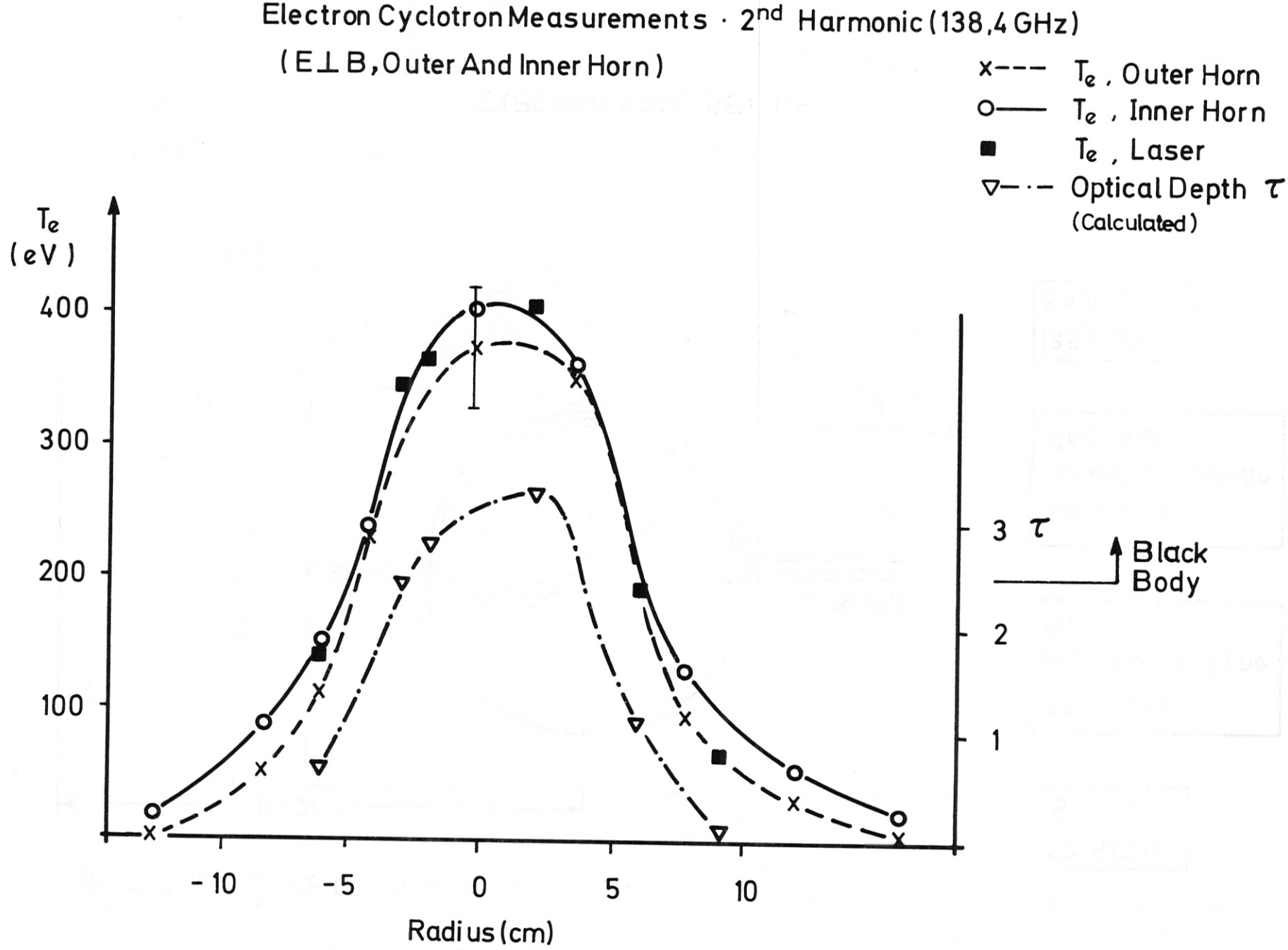
Electron Cyclotron Measurements · 2nd Harmonic (138,4 GHz)
(E⊥B, Outer And Inner Horn)
x--- Te , Outer Horn
o—— Te , Inner Horn
■ Te , Laser
▽-·- Optical Depth τ
(Calculated)
Te
(eV)
400
300
200
100
3 τ
Black
Body
2
1
-10
-5
0
5
10
Radius (cm)

Figure 3

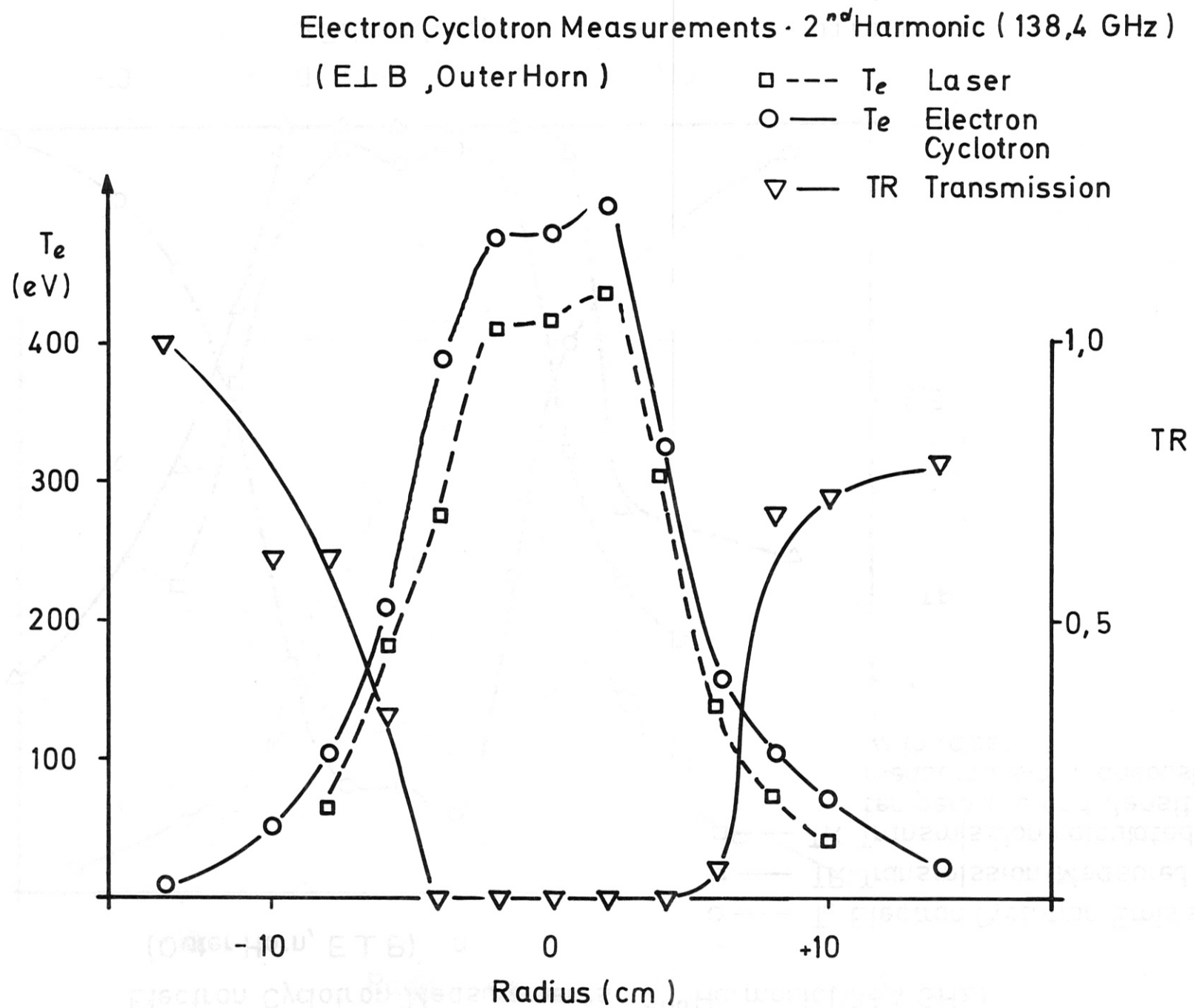
Electron Cyclotron Measurements · 2nd Harmonic (138,4 GHz)
(E⊥ B , Outer Horn)
□ --- Te Laser
○ — Te Electron Cyclotron
▽ — TR Transmission
Te (eV)
400
300
200
100
1,0
0,5
TR
-10
0
+10
Radius (cm)

Figure 4

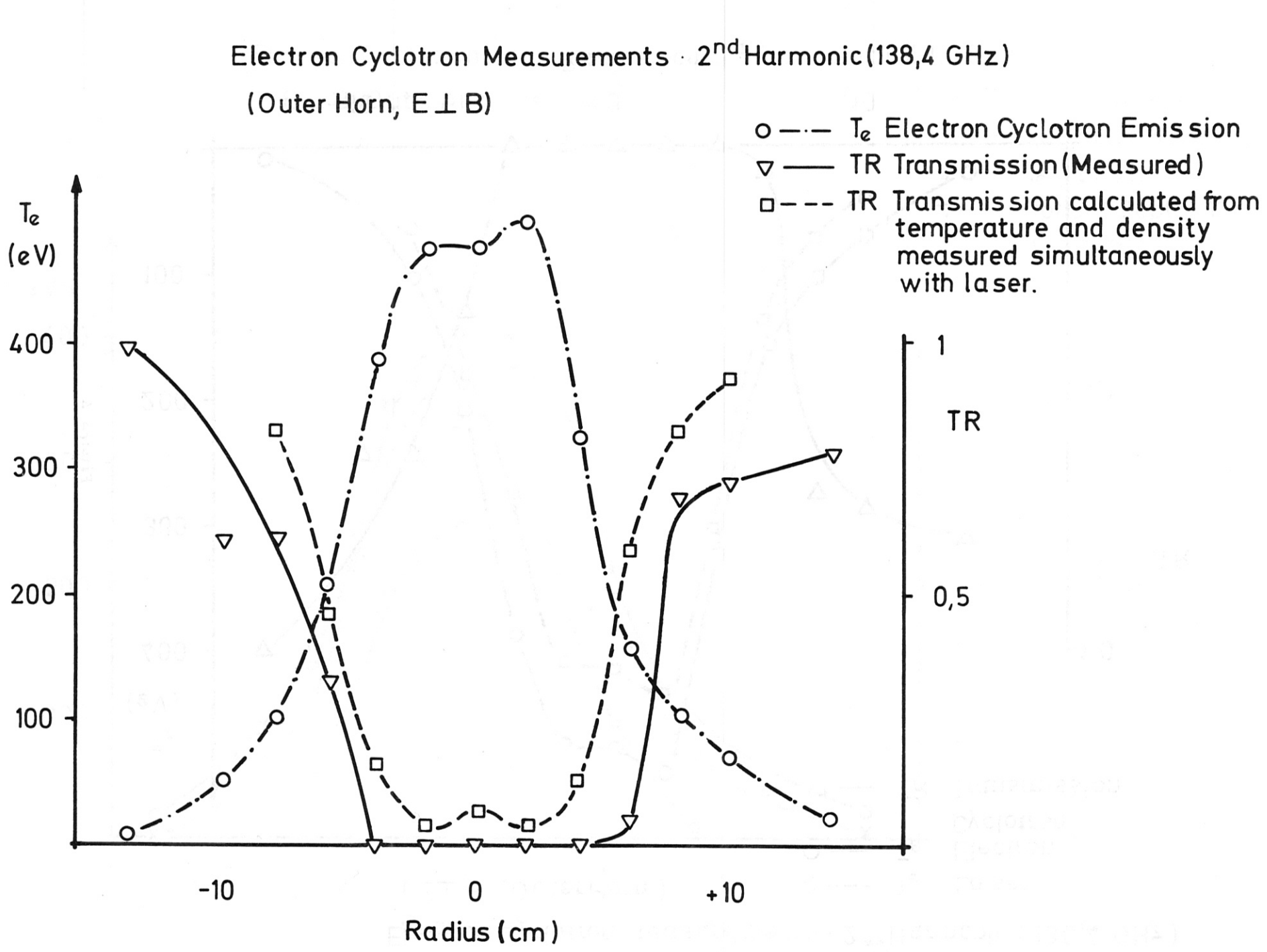
Electron Cyclotron Measurements · 2nd Harmonic (138,4 GHz)
(Outer Horn, E ⊥ B)
o —·— Te Electron Cyclotron Emission
▽ —— TR Transmission (Measured)
□ - - - TR Transmission calculated from temperature and density measured simultaneously with laser.
Te (eV)
400
300
200
100
1
TR
0,5
-10
0
+10
Radius (cm)

Figure 5

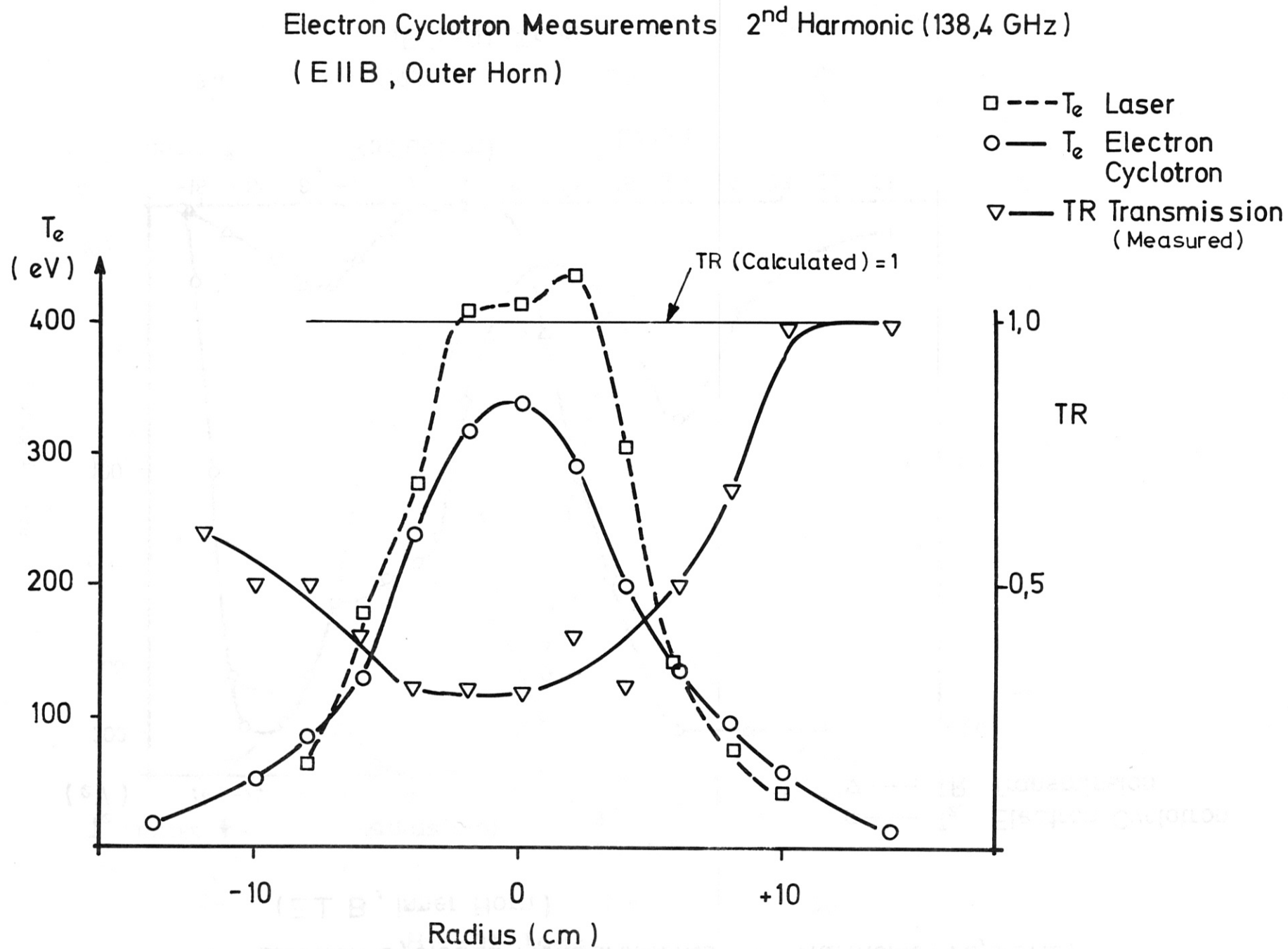
Electron Cyclotron Measurements 2nd Harmonic (138,4 GHz)
(E II B , Outer Horn)
□ --- Te Laser
○ — Te Electron Cyclotron
▽ — TR Transmission (Measured)
Te (eV)
400
300
200
100
TR (Calculated) = 1
1,0
0,5
TR
-10
0
+10
Radius (cm)

Figure 6

Electron Cyclotron Measurements · 1st Harmonic (72,5 GHz)

(E ⊥ B , Inner Horn)

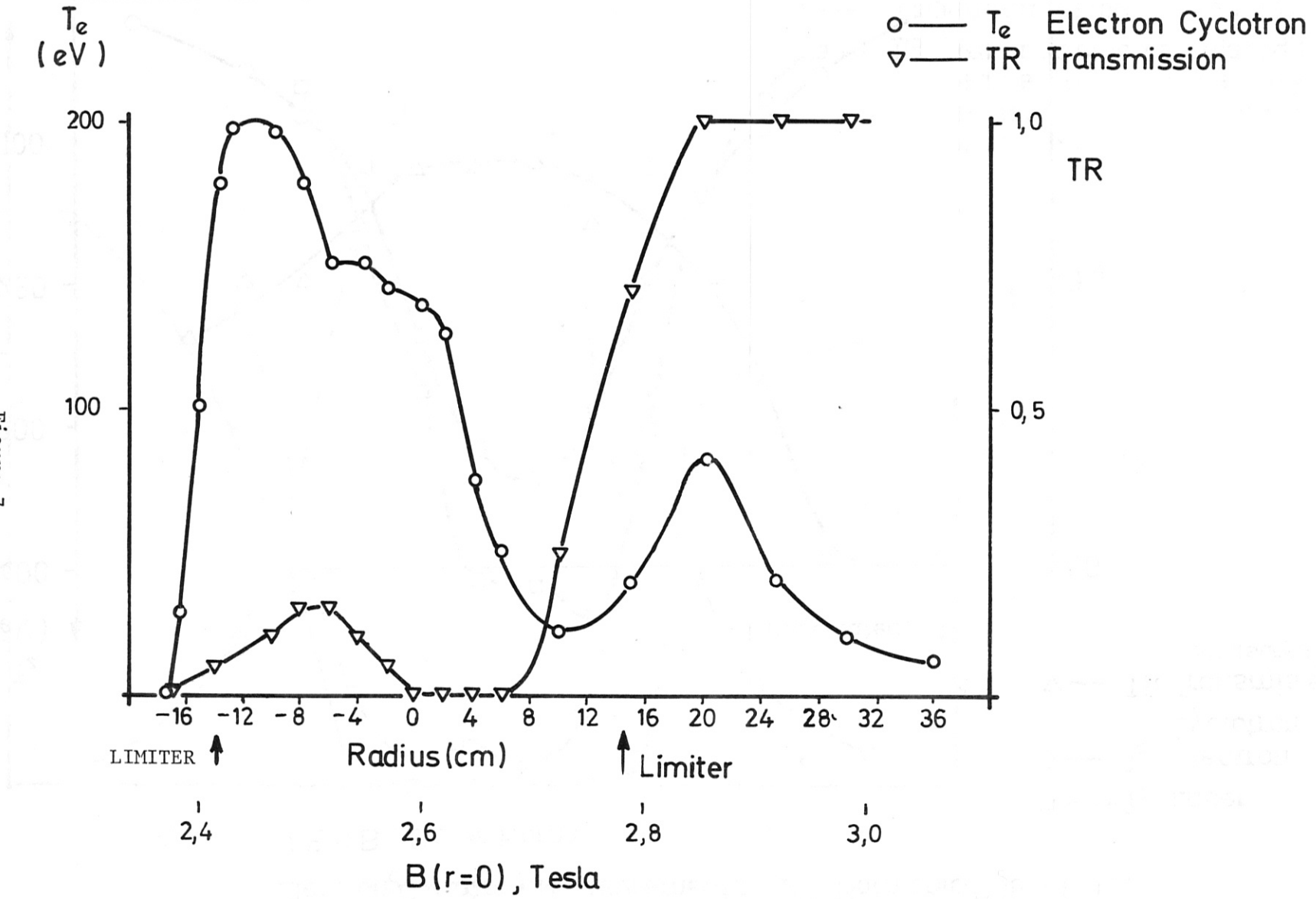

Figure 7

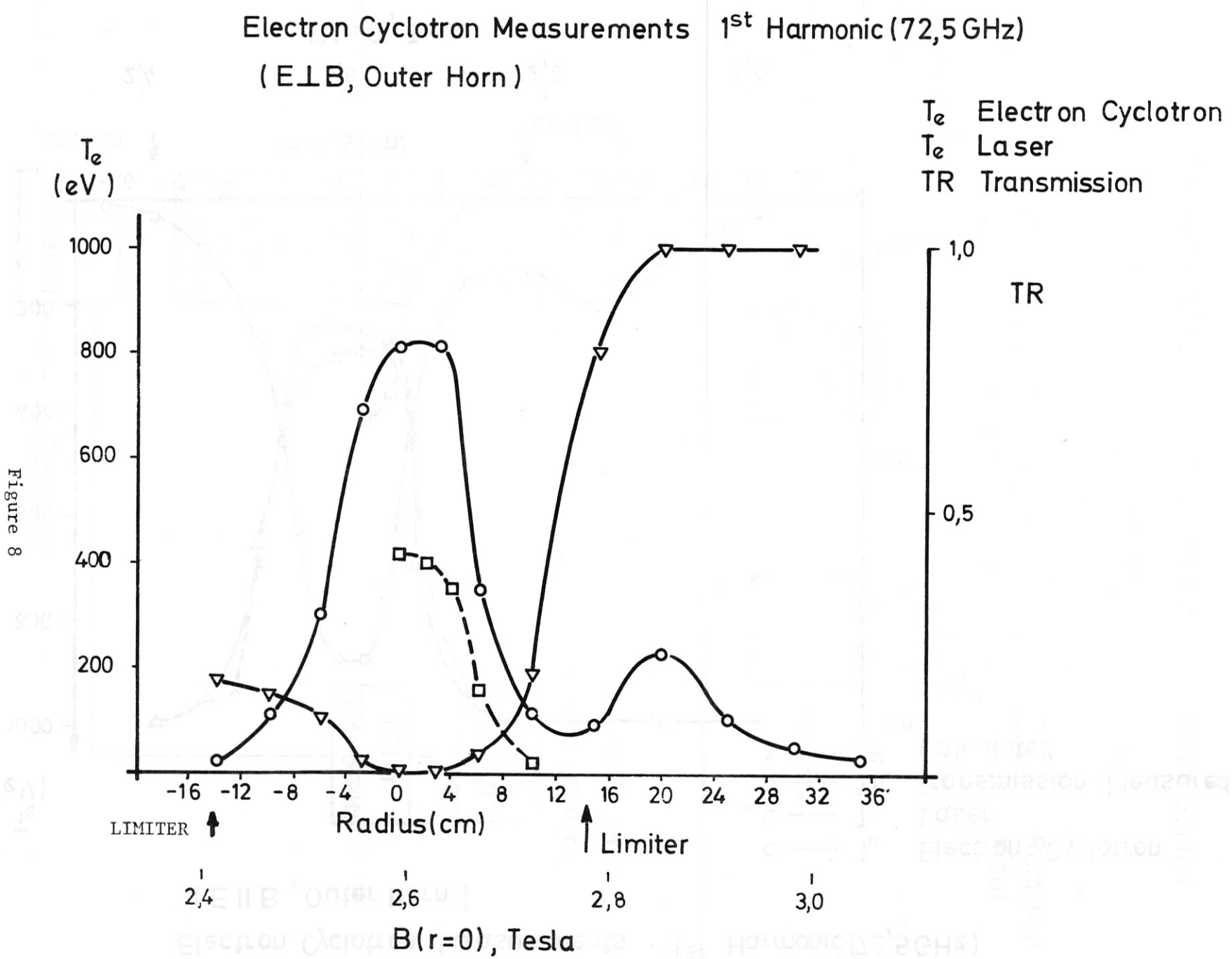
Electron Cyclotron Measurements 1st Harmonic (72,5 GHz)
(E⊥B, Outer Horn)
Te Electron Cyclotron
Te Laser
TR Transmission
Te
(eV)
1000
800
600
400
200
1,0
0,5
TR
-16 -12 -8 -4 0 4 8 12 16 20 24 28 32 36
LIMITER
Radius(cm)
Limiter
2,4
2,6
2,8
3,0
B(r=0), Tesla

Figure 8

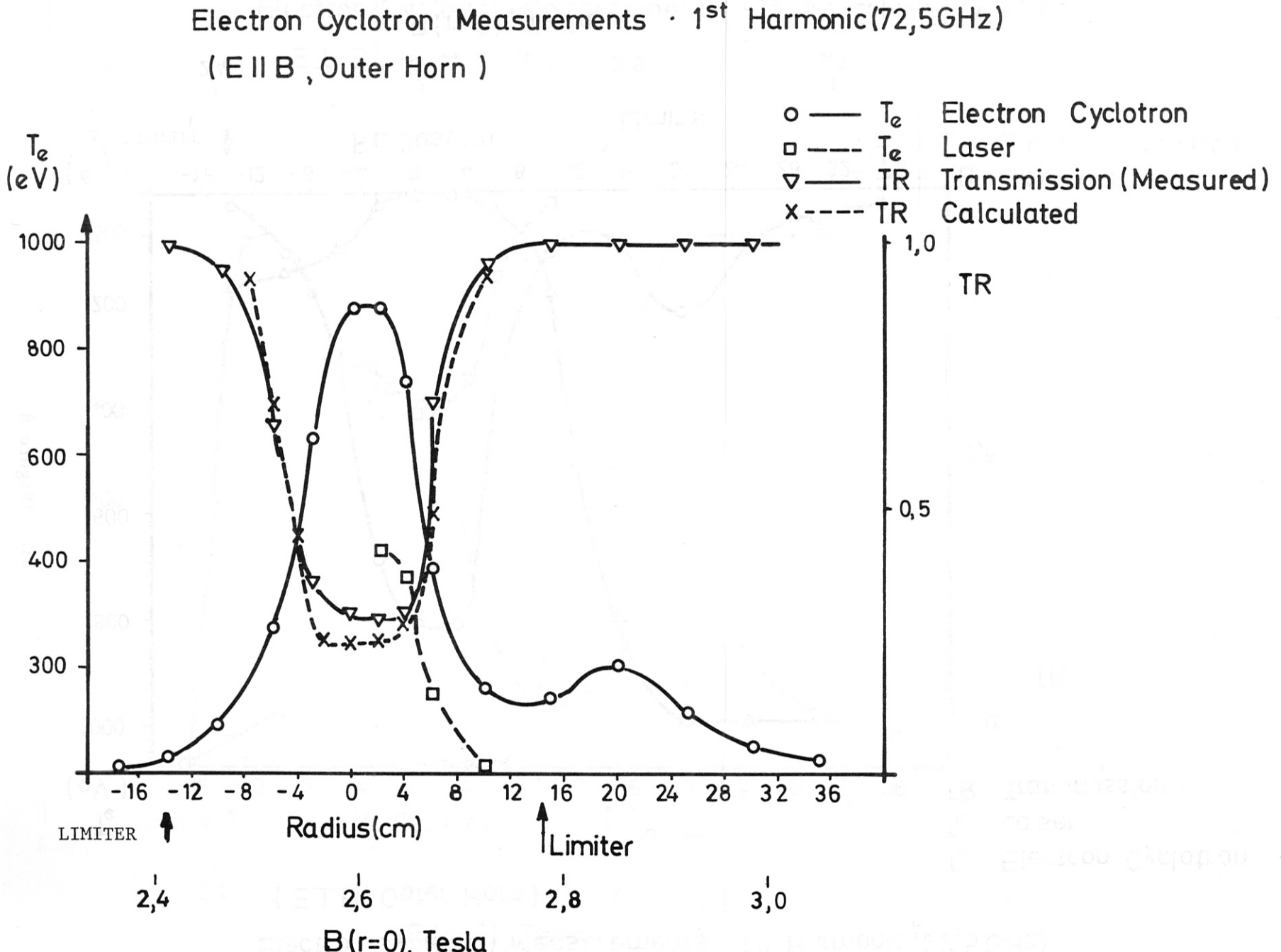
Electron Cyclotron Measurements · 1st Harmonic (72,5 GHz)
(E II B , Outer Horn)
o —— Te Electron Cyclotron
□ --- Te Laser
▽ —— TR Transmission (Measured)
x ---- TR Calculated
Te (eV)
1000
800
600
400
300
1,0
TR
0,5
-16 -12 -8 -4 0 4 8 12 16 20 24 28 32 36
LIMITER
Radius(cm)
Limiter
2,4 2,6 2,8 3,0
B (r=0), Tesla

Figure 9

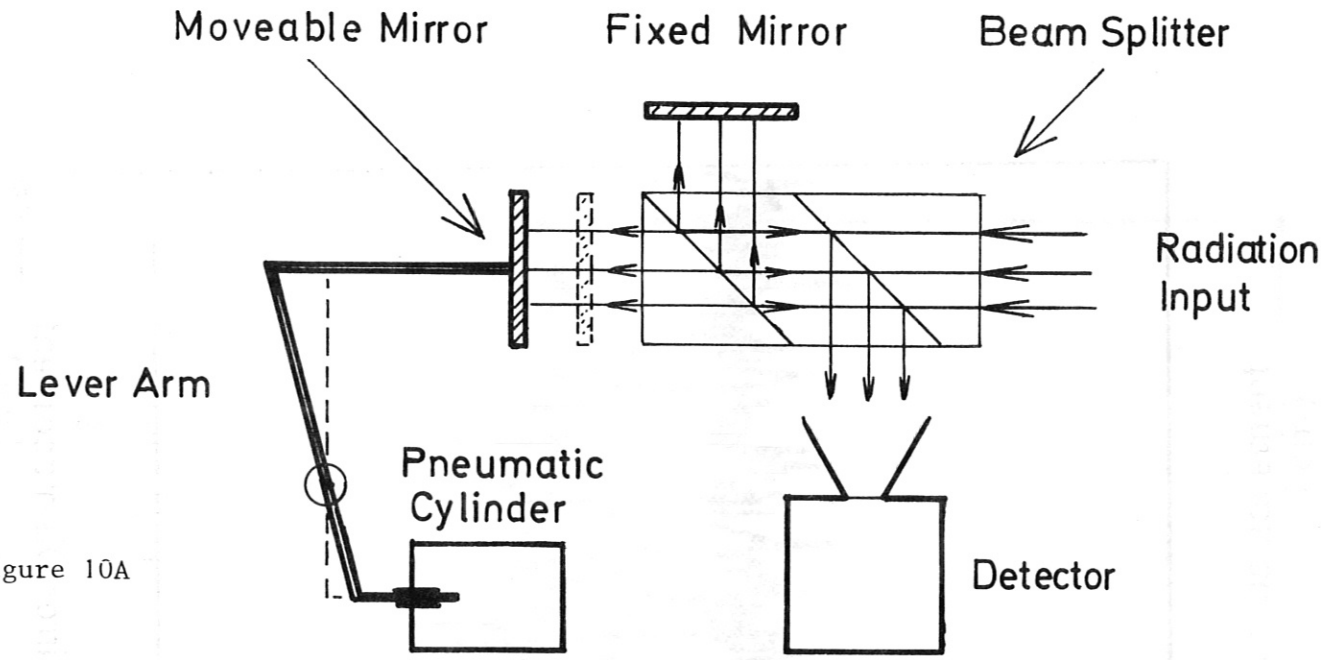

Figure 10A

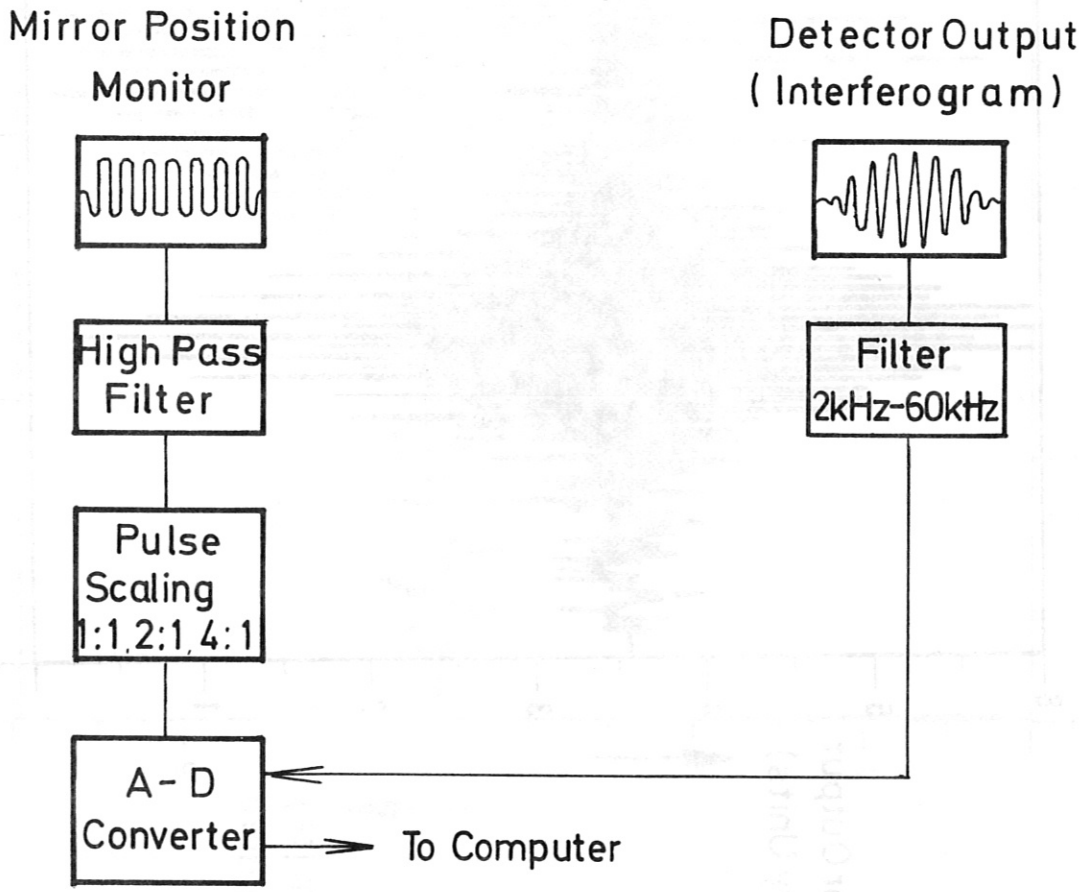

Figure 10B

Figure 10

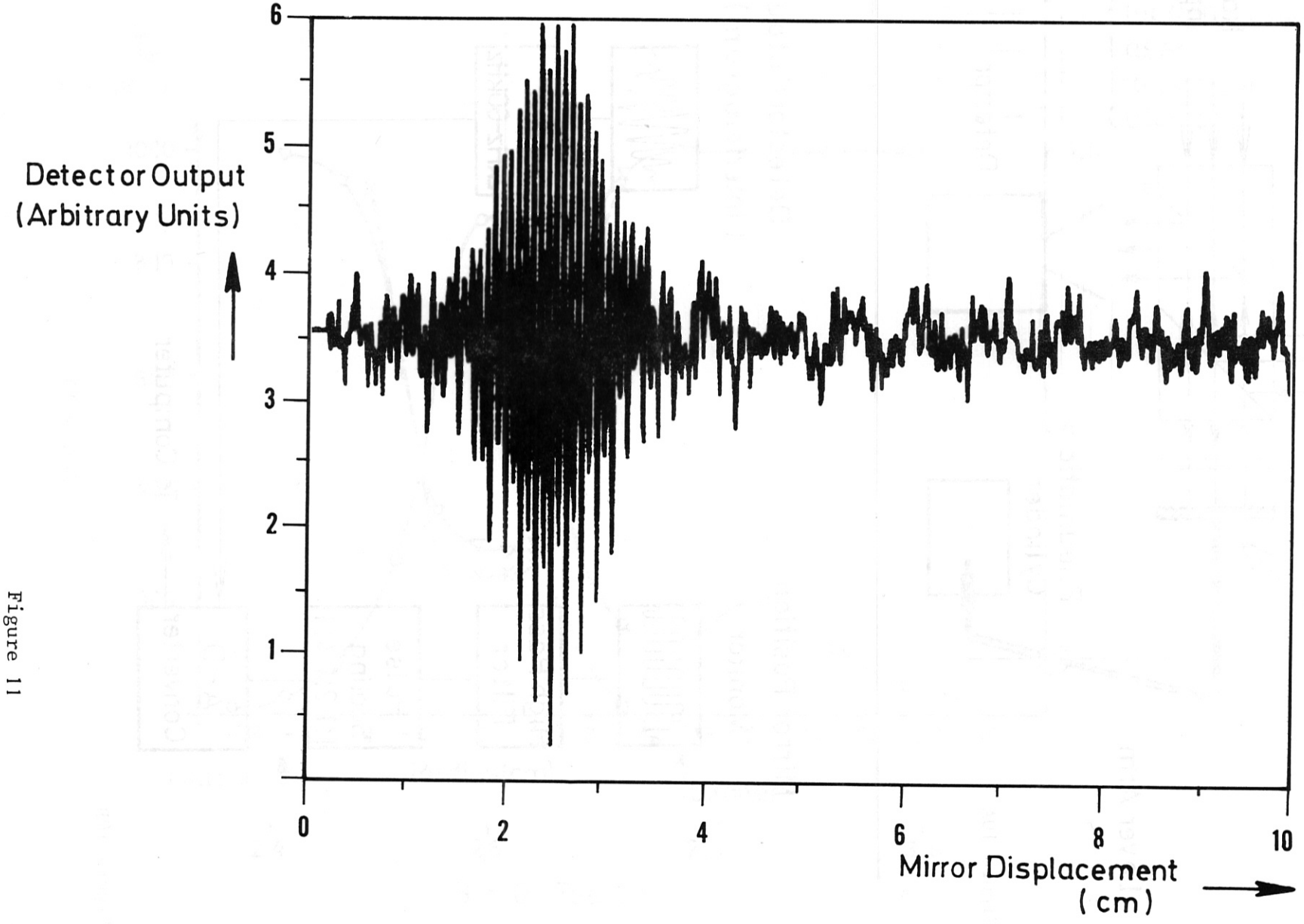
Detector Output
(Arbitrary Units)
6
5
4
3
2
1
0
2
4
6
8
10
Mirror Displacement
(cm)

Figure 11

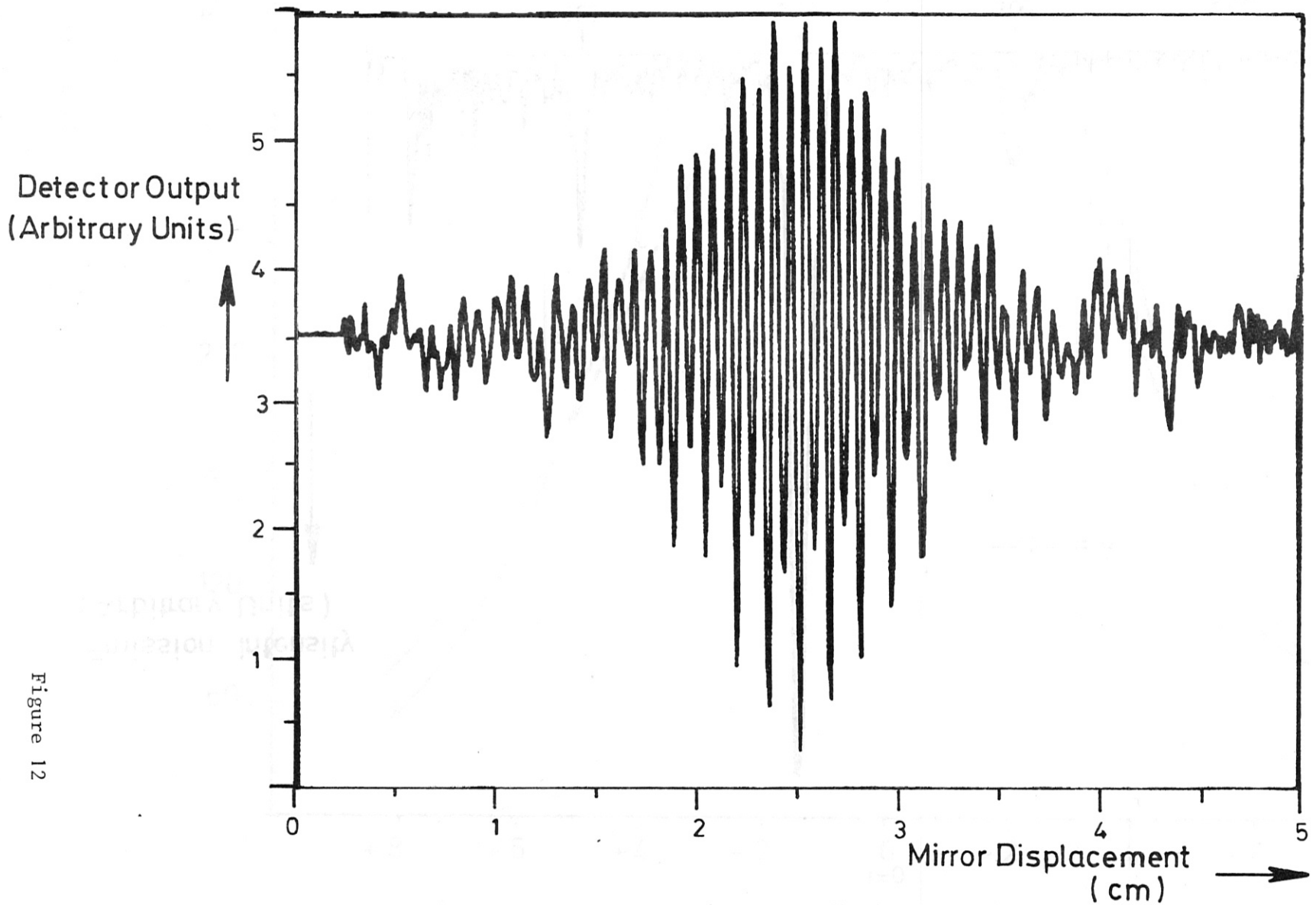
Detector Output
(Arbitrary Units)
1
2
3
4
5
0
1
2
3
4
5
Mirror Displacement
(cm)

Figure 12

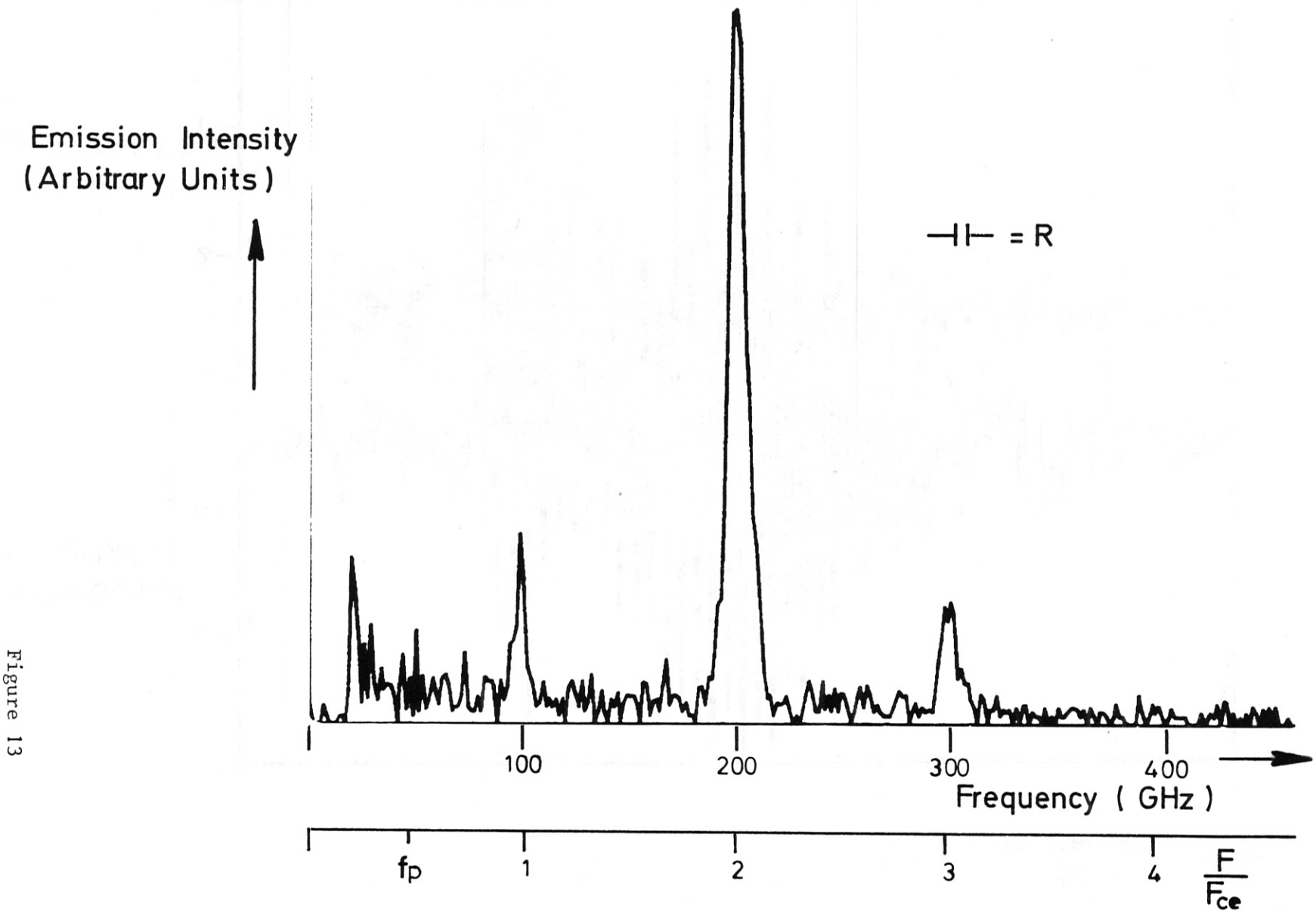
Emission Intensity
(Arbitrary Units)
⊣|⊢ = R
100
200
300
400
Frequency (GHz)
fp
1
2
3
4
F
Fce

Figure 13

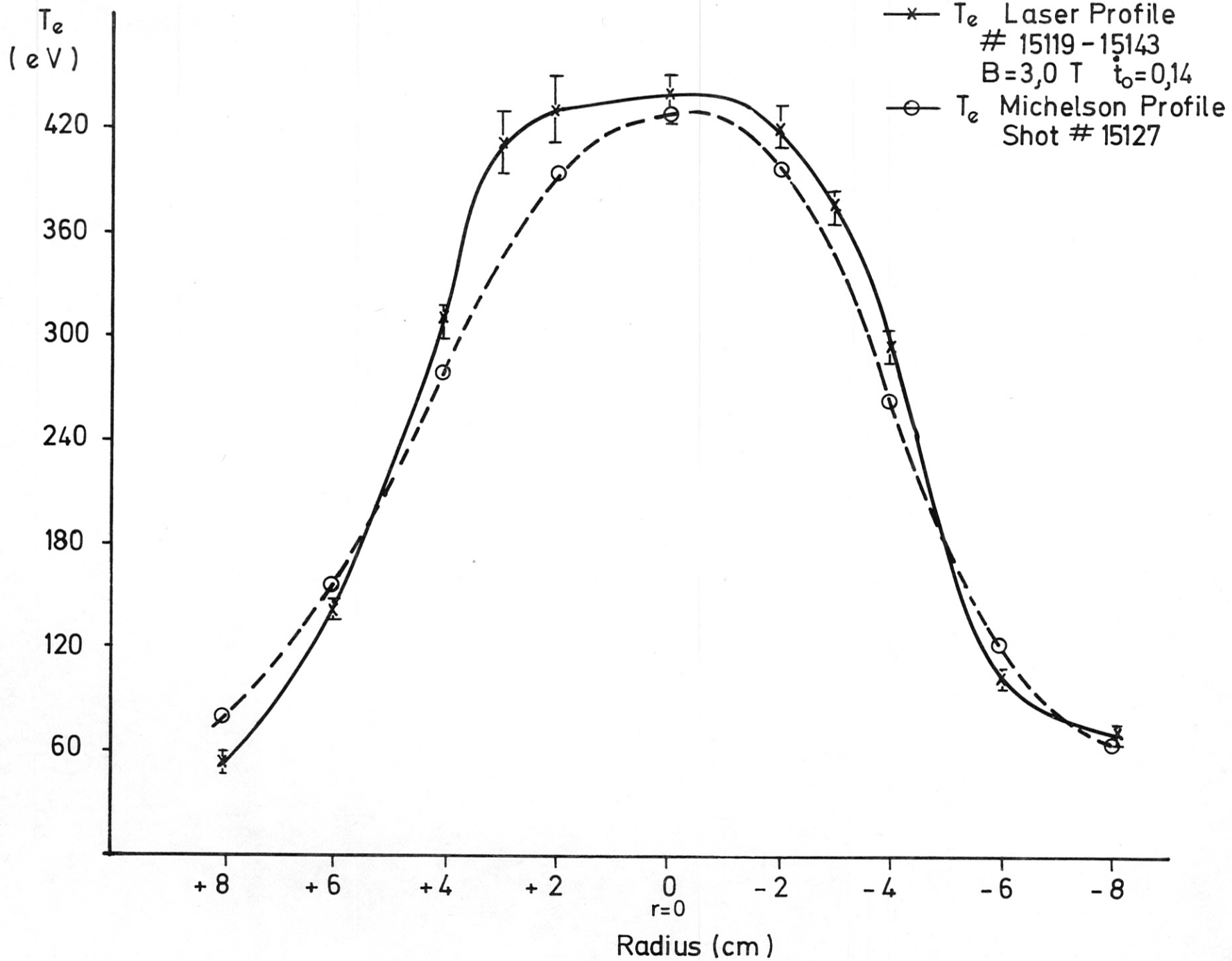
T_e (eV)
420
360
300
240
180
120
60
+8
+6
+4
+2
0
r=0
-2
-4
-6
-8
Radius (cm)
T_e Laser Profile
# 15119 - 15143
B=3,0 T $\dot{t}_o$=0,14
T_e Michelson Profile
Shot # 15127

Figure 14